Vol 14 No 3, March 2005
1009-1963/2005/14(03)/0586-06

Chinese Physics

© 2005 Chin. Phys. Soc.
and IOP Publishing Ltd

The synthesis of one-dimensional controllable ZnO microrods*

Zhang Lin-Li(张琳丽)[a)b)†], Guo Chang-Xin(郭常新)[a)b)],
Chen Jian-Gang(陈建刚)[b)], and Hu Jun-Tao(胡俊涛)[b)]

[a)] *Structure Research Laboratory, University of Science and Technology of China, Hefei* 230026, *China*

[b)] *Department of Physics, University of Science and Technology of China, Hefei* 230026, *China*

(Received 15 July 2004; revised manuscript received 10 November 2004)

Various morphology ZnO submicrorods and microrods have been fabricated onto glass substrates through chemical solution growth by the source of zinc acetate ($Zn(CH_3COO)_2{\cdot}2H_2O$) and hexamethylene tetraamine ($(CH_2)_6N_4$). We discuss the influence of PH and the concentration of the solution on the shapes of the as-synthesized ZnO samples. And analyse the growth mechanism. The regular hexagonal ZnO rods align has been made by control of a certain concentration and proper PH. The hexagonal ZnO columns mainly grew in the [002] direction. X-ray diffraction (XRD), scanning electron microscopy (SEM) and photoluminescence (PL) are used to characterize the structure, the morphology and optical property of the samples. The photoluminescence spectrum of hexagonal ZnO columns shows that there are a broad strong red band (650nm) and a broad band in short wavelength which are two overlapped emission bands with the peaks at about 380nm and 430nm.The UV emission (∼387nm) comes from recombination of free excitons. The blue emission with peak at 430nm is assigned for the recombination from an electron at interstitial Zn to a hole in VB. The red emission at 650nm is ascribed to the recombination from an electron at Vo^{2+} to a hole in VB.

Keywords: ZnO, microrods, photoluminescence, crystallite growth, chemical solution method
PACC: 7280E, 8110D, 7855E, 7840G

1. Introduction

In the past decade, due to the strong commercial desire for ultraviolet (UV) and blue optical devices, great interest has been focused on the synthesis and optical properties of wide-band-gap semiconductors.[1−3] ZnO, a II–VI compound semiconductor with a wide and direct band gap of 3.37eV at room temperature, has been recognized as a good candidate for use in blue and UV light emission and room temperature optical UV lasing because of its large exciton binding energy (60 meV), which is much greater than that of GaN (25meV) and the electron thermal excited energy at room temperature (26meV). So exciton at room temperature exists and adapts to room temperature UV lasing. It is applicable to use in low-voltage and short-wavelength electro-optical devices such as light-emitting diodes and diode lasers.[1−6] Its other applications include ones in transparent ultraviolet protection films, chemical sensors[7] and solar cells.[8] More recently, a great deal of attention has been focused on the fabrication of one-dimensional ZnO nanomaterials.

The synthesis includes chemical and physical routes, which need special devices, and the process is complicated. Also the cost is high. It is relatively simple to use chemical ones as compared to physical methods. Relatively perpendicularly orientated ZnO rods have been prepared in a two-step solution deposition approach.[9] But this requires growth in two different solutions in turn and the conditions of growth in the two solutions are distinct. In this paper, a simple one-step and convenient chemical bath method has been used to synthesize one-dimensional ZnO rods. The aim of this study is to prepare the controllable ZnO align by control of a certain concentration and proper PH. Preparing ZnO with this method has the advantages of simple equipment, operating conveniently and low cost, so it has a great future in making one-dimensional ZnO.

*Project supported by the Anhui Nature Science Foundation (Grant No 01044904) and the National Natural Science Foundation of China (Grant No 19874057).

†E-mail: guocx@ustc.edu.cn

2. Experiments

ZnO microrods were grown onto glass plate substrates through a chemical solution deposition system. In experiments the raw materials are zinc acetate ($Zn(CH_3COO)_2{\cdot}2H_2O$) and hexamethylene ($(CH_2)_6N_4$), microscope carrying glass plates as substrates. The glass plate pretreatment was as follows: first, the glass plates were scraped by cotton with ether; they were then cleaned by an ultrasonic instrument in alcohol for 5h and dipped in acetone for half an hour, and finally, washed with deionized water. In the experiment, the molar concentration ratio of $(Zn(CH_3COO)_2{\cdot}2H_2O)$ to $((CH_2)_6N_4)$ was 1:1, while the concentration of each raw material was 0.1M or 0.01M. Aqueous solutions of HCl and NaOH were used to adjust the value of PH. The cleaned glass plates were placed on the bottom of the beaker, which was heated at a constant temperature for different time (about 1–10h) in a constant lab water bath. White ZnO thin layers were grown on the substrates with the increasing growth time. Finally, the as-prepared ZnO products were washed with deionized water and dried in air at room temperature.

The as-grown samples were characterized in a variety of ways. X-ray diffraction (XRD) was conducted on a Rigaku D/MAX-rA diffractometer with Cu Kα(λ=0.15418nm) as the incident radiation at room temperature. Scanning electron microscopy (SEM) photographs were taken by a model of Hitachi X-650. Photoluminescence (PL) spectra were performed on a Hitachi 850-type fluorescence spectrophotometer with a Xe lamp as the excitation light source at room temperature.

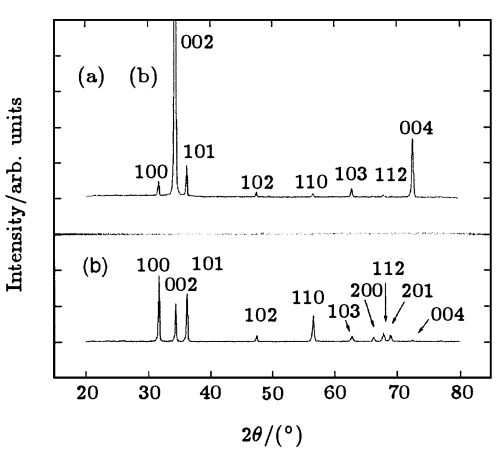


Fig.1. X-ray diffraction diagram of ZnO samples (the reaction condition is: the mole ratio of raw materials $Zn(CH_3COO)_2{\cdot}2H_2O$ to $(CH_2)_6N_4$=1:1, PH=6, the growth time of 6h, the concentration of raw materials: (a) 0.1M sample 1# and (b) 0.01M sample 2#).

3. Results and discussion

3.1. XRD measurements

XRD patterns of the as-prepared ZnO rods are shown in Fig.1. The preparation condition is: PH=6, the growth time of 6h, the concentration of raw materials: (a) sample 1# 0.1M and (b) sample 2# 0.01M. According to the JCPDS file, the two diagrams indicate that all the x-ray patterns in the ZnO rods are assigned to a typical wurtzite phase structure. The lattice constants calculated from the peaks are a=0.3257nm, c=0.5205nm (1#) and a=0.3253nm, c=0.5260nm (2#). It can be concluded that the value of lattice parameter a gets larger and that of c gets smaller when samples prepared in high concentration solution. From Fig.1(b), it can be seen that the ratio of intensities of peaks corresponds to that of typical ZnO powder. The three strong peaks appear at 2θ=31.78°, 34.4°, 36.22°, assigned to the ZnO (100), (002), (101), respectively. Other weak peaks in turn are ZnO planes (102), (110), (103), (200), (112), (201) and (004), where (200) and (004) are the second order diffractions of planes (100) and (002), respectively. In contrast (Fig.1(a)), the diffraction peaks of planes (100) and (101) become very weak, while the (002) peak grows intense and sharp and the (004) peak occurs and grows intense. Generally, the preferential c-axis orientation can be indicated by the ratio of intensities of (00l) peaks to that of all peaks. While the film is highly oriented in a direction, the peaks of certain planes will intensify and others will be weaker. To the ZnO microrods, the peak of the strongest diffraction corresponds to plane (002), which occurs at 2θ=34.4° and the stronger peak of plane (004) is the second order diffraction of plane (002). The occurrence of peak (004) accompanied with peak (002) means preferential orientation of ZnO rods in the c-axis direction.

3.2. SEM analysis

3.2.1. The concentration of solution

Figure 2 shows the SEM micrographs of the as-synthesized ZnO obtained under the same temperature, growth time and PH values, but different concentrations. Sample 1# is the hexagonal ZnO rods parallel align as shown in Fig.2(a). The hexagonal rods are perfectly regular and almost perpendicular to the glass substrate, which are consistent with the above XRD results that indicated ZnO rods are [002]

preferred growth orientation. The perfectly hexagonal end plane of ZnO rods with the diameter of about 4–6μm is a plane surface and perpendicular to the growth axis *c*. The ratio of length to diameter is approximate to 5. The inset in Fig.2(a) is a big grain that we selected. It has regular shape. A low magnification SEM of forked lathy ZnO rods (Sample 2#) is shown in Fig.2(b). The lengths and widths are not uniform. The length is in the range of 18–28μm and the diameter is about 0.8–1.5μm. The ratio of length to diameter is about 18–32. It is special that the end plane of some rods has split into many thin rods at the end. And the thin end surface is still hexagonal plane. It can be induced that when the concentration of the solution is lower, the ratio of length to diameter of ZnO rods is relatively greater and they grow neither perpendicularly to the substrate nor along the substrate but in disorder. This result is consistent with the forenamed XRD data.

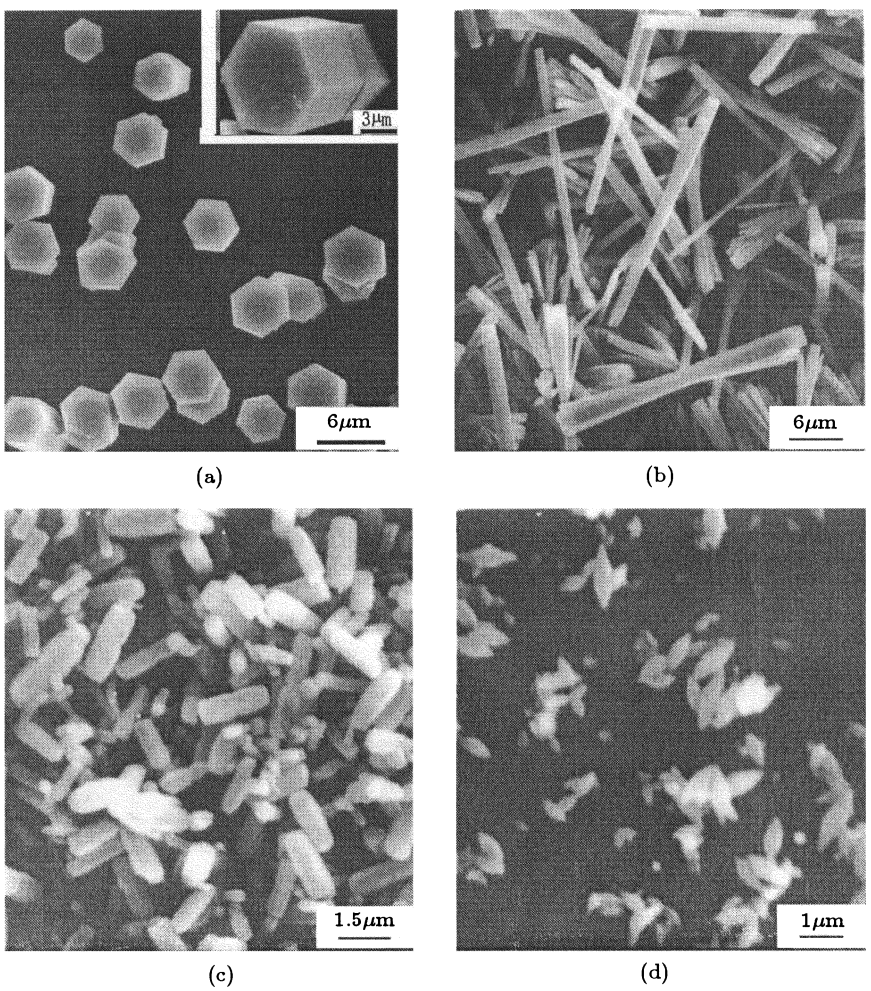


Fig.2. SEM photographs of ZnO samples (the concentration of raw materials $Zn(CH_3COO)_2{\cdot}2H_2O$ and $(CH_2)_6N_4$, the PH values and the growth time are respectively (a) 0.1M, PH=6, 6h sample 1#, (b) 0.01M, PH=6, 6h sample 2#, (c) 0.01M, PH=7.5, 6h, (d) 0.01M, PH=8.6, 6h).

3.2.2. The influence of the value of PH

Figure 2(b)–(d) show SEM images, which correspond to products deposited on the same concentration (0.01M) and the same growth time (6h) but different PH. Sample 2# has a mean length of 23μm and a diameter of below 1.5μm in Fig.2(b). Sample 3# in Fig.2(c) are short one-pair rods grown symmetrically from a centre to both sides. Its diameter is in the range of 0.4–1μm and length is about 1.5–2μm. This shape (spindly rods) in Fig.2(c) is different from the regular hexagonal rods with the same cross section in Fig.2(a). With the growth time increasing, its diameter of cross section grows shorter and the hexagonal section becomes circle-like. Eventually when the PH value increases to 8.6, it becomes olive-core at both ends of rods as given in Fig.2(d). From the foregoing

comparison, it can be concluded that when the value of PH varies from 6 to 7.5, the length of the samples gets shorter, the diameter diminishes and the ratio of length to diameter gets smaller. This kind of microrod growth behaviour is consistent with that of ZnO single crystal in aqueous solution.[10,11]

The growth mechanism of ZnO microrods is as follows: ZnO is a polar crystal, whose polar axis is the c-axis. In ZnO structure, each Zn atom is surrounded by four O atoms, which forms the tetrahedral configuration. Zn leans to the (0001) face and O leans to the $(000\bar{1})$ face. In the theoretic model of anionic coordination polyhedra, growth units are the complex $[Zn(OH)_4]^{2-}$, which Zn^{2+} ions situated in the centre of tetrahedron and OH^- situated in the four vertices. In the supersaturation solution, due to the diffusion of ions, and deregulation movement among molecules and ions, growth units $[Zn(OH)_4]^{2-}$are bonded together through a dehydration reaction ($OH^- + OH^- = H_2O + O^{2-}$) forming ZnO hexagonal structure. As the growth velocities of each plane in crystal are different, the crystal face whose growth rate is slow easily appears while the crystal face whose growth rate is fast easily disappears. And the extent of appearance of the positive and negative crystal facets are different due to the diverse growth conditions.[12,13] In high temperature and strong alkaline medium, the chance that growth units integrated into each crystal facet is almost the same. The shape of micro-crystallites is short columnar or polyhedral form, while in relatively low temperature and weak alkaline or acid or neutral medium, it has the shape of hexagonal long column shown in Fig.3. The relationship between the grow habits of ZnO microcrystallites and the growth conditions are shown in Fig.4. Figure 4 shows that with the concentration or PH of solution, the shapes of ZnO are getting from long column to olive-core. So the top plane $(000\bar{1})$ easily formed into regular hexagonal plane and side planes $\{01\bar{1}0\}$ easily formed into column faces. When the count of OH^- ions in the solution corresponds to that of Zn^{2+} ions, the shape of ZnO is long column (Fig.2(b)) and when the count of OH^- ions goes on increasing, the shape becomes short column. With the value of PH increasing, the growth velocity in c-axis decreases and the shape of sample gradually tend to be spindly (Fig.2(c)) and olive-core (Fig.2(d)). When PH reaches a certain value, it becomes grainy. It can be clearly seen that ZnO rods grow from one centre to both sides in Fig.2(c). And we can also clearly see that there is a deep color ring in the middle of this hexagonal rod. In fact, two growth units (Fig.3(b)) grown symmetrically from one positive plane (0001) to both sides along $+c$ and $-c$ axis form such image at tip end plane (Fig.2(a)). We think the centre is the (0001) plane. During the growth, it is Coulomb repulsion that makes two growth units (Fig.3(b)) symmetrically grow from one positive plane (0001) to both sides.

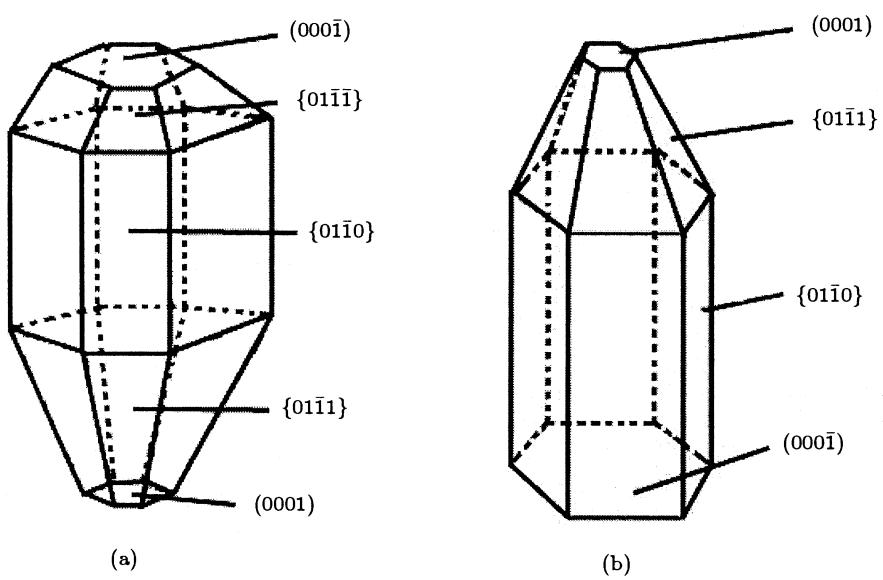


Fig.3. The growth habits of ZnO in solution (a) strong alkaline solution (b) weak alkaline solution.

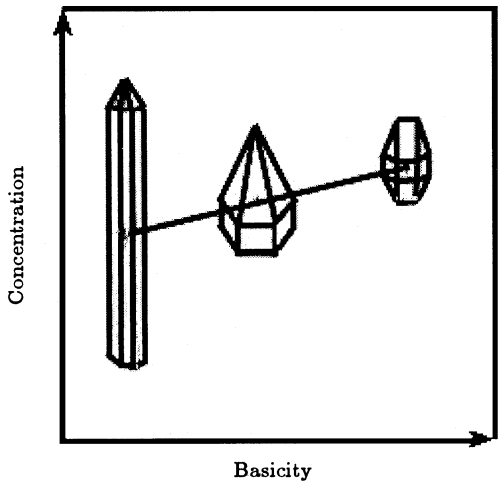


Fig.4. The relationship between the growth habits of ZnO micro-crystallites and the growth conditions.

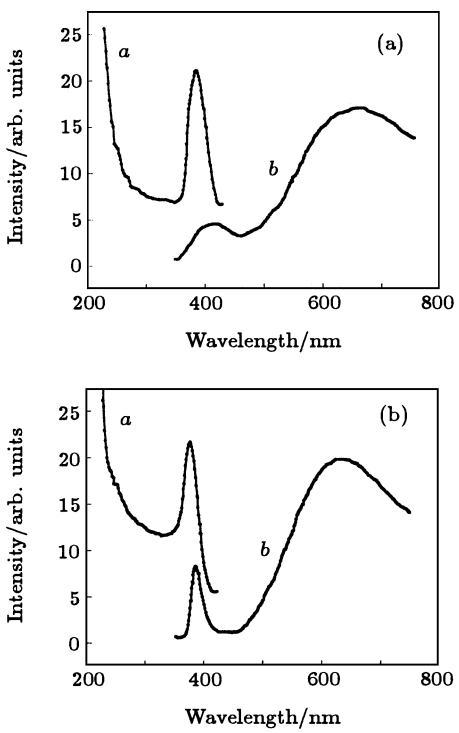


Fig.5. (a) PL of 1# sample curve *a* excitation spectrum (λ_{em}=650nm) and curve *b* emission spectrum (λ_{ex}=325nm) (b) PL of 2# sample curve *a* excitation spectrum (λ_{em}=650nm) and curve *b* emission spectrum (λ_{ex}=325nm).

3.3. Photoluminescence measurements

Photoluminescence (PL) spectra of ZnO microrods under different growth conditions at room temperature excited by Xe lamp are shown in Fig.5. Figure 5(b) shows the excitation and emission spectra of sample 2#. In excitation spectrum, when the detected wavelength is 650nm, besides the intrinsic interband excitation, there is an exciton peak at 380nm with FWHM about 23nm at room temperature and a turnup in the range of 200–250nm for there is an excitation peak at 195nm.[14] When the excited wavelength is 325nm, it is clear that the spectra consist of a narrow weak peak in the near-UV region and a broad strong peak in the visible region in the curve *b* of Fig.5(b). The UV emission peak is at 387nm and the visible emission peak is about 650nm with FWHM about 250nm. We compared the PL and excitation spectra of sample 1# (Fig.5(a)) with that of sample 2# (Fig.5(b)). When the concentration of the solution is increasing from 0.01M to 0.1M, a strong broad red-orange emission at 650nm is similar in the PL spectra. But the width of the UV emission peak at 387nm gets larger. In fact, it is two overlapping emission bands with the peaks located at about 380nm and 430nm. The excitation spectra of sample 2# and sample 1# are also similar. Only the excitation spectrum of sample 1# gets larger. We suggest that the above change is derived from the excessive defects of Zni in higher concentration of the solution. The UV emission (~387nm) comes from recombination of free excitons. However, the assignment of the observed transitions in the literature is controversial, which is partly due to the fact that the nature of the observed transitions depends sensitively on the preparation conditions. Generally, oxygen vacancies act as the so-called luminescence centres.[15–18] There are three charge states of oxygen vacancies: Vo^0, Vo^+ and Vo^{2+}. According to Ref.[15], the positions of oxygen vacancies lie below the bottom of CB from top to bottom are Vo^0, Vo^+ and Vo^{2+} in turn and only Vo^+ is paramagnetic. In EPR experiments, the signal of its EPR can be detected. Xu has been calculated the level position of intrinsic point defects and its complex using full potential linear Muffin-tin orbital (FP-LMTO) method.[16] The result shows that vacant Zn (Vzn) and interstitial O (Oi) produce shallow acceptor levels at 0.3eV and 0.4eV above the top of VB. Interstitial Zn (Zni) produces a shallow donor level at 0.5eV below the bottom of CB. It was also calculated that a deep donor level at 1.3eV below the bottom of CB is Vo^{2+}. According to Ref.[19,20], Vo^+ lies around 2.4eV at the bottom of CB. A simple chart has been drawn as shown in Fig.6. As indicated by the PL spectrum in curve *b* of Fig.5(a), the emission at 430nm is assigned to the recombination from an electron at Zni to a hole in VB. The red emission at 650nm is ascribed to the recombination from an electron at Vo^{2+} to a hole in VB.

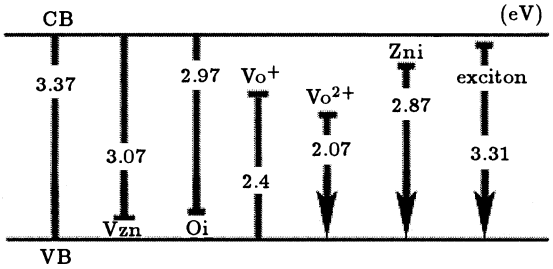


Fig.6. The intrinsic defect state levels of ZnO (Ref.16,19,20).

4. Conclusion

Various morphology of ZnO microrods such as perfectly regular hexagonal column rods, forked lathy hexagonal rods, hexagonal spindly rods grown symmetrically from a centre to both sides, and olive-core rods have been synthesized on glass substrate through chemical solution approach by the raw material of zinc acetate ($Zn(CH_3COO)_2{\cdot}2H_2O$) and hexamethylene ($(CH_2)_6N_4$). The shapes vary with the PH value. In weak acid medium, it is lathy. However, in a weak alkaline medium, it is of one-pair rods. With increasing of concentration of solution, the ratio of length to diameter decreases and ZnO rods on glass substrate prefer to be perpendicular to substrate rather than be in disorder. So we can fabricate highly oriented regular hexagonal ZnO rods by control of a certain raw material concentration and proper PH value. The photoluminescence spectrum of highly oriented regular hexagonal ZnO rods shows that there is a broad strong red band (650nm) and a broad band in short wavelength which are two overlapping emission bands with the peaks at about 380nm and 430nm. However, the emission spectrum of lathy ZnO rods shows a broad red band with peak at around 650nm and FWHM of about 250nm and a narrow weak UV peak (~387nm) when the excited wavelength is 325nm. The UV emission (~387nm) comes from the recombination of free excitons. The blue emission with peak at 430nm is assigned to the recombination from an electron at Zni to a hole in VB. The red emission at 650nm is ascribed to the recombination from an electron at Vo^{2+} to a hole in VB.

References

[1] Li Y, Meng G W, Zhang L D and Phillipp F 2000 *Appl. Phys. Lett.* **76** 2011

[2] Lin B X, Fu Z X, Jia Y B *et al* 2001 *Acta Phys. Sin.* **50** 2208 (in Chinese)

[3] Yuan H T, Zhang Y and Gu J H 2004 *Acta. Phys. Sin.* **53** 646 (in Chinese)

[4] Wong E M and Searson P C 1999 *Appl. Phys. Lett.* **74** 2939

[5] Bagnall D M, Chen Y F, Zhu Z, Yao T, Koyama S, Shen M Y and Gato T 1999 *Appl. Phys. Lett.* **70** 2230

[6] Guo X L, Choi J H, Tabata H and Kawai T 2001 *Jpn. J. Appl. Phys.* Part 2 **40** L177

[7] Sberveglieri G, Groppelli S, Nelli P, Tintinelli A and Giunta G 1995 *Sensors Actuators.* B **25** 588

[8] Devaney W E, Chen W S, Stewart J M and Mickelsen R A 1990 *IEEE Trans. Electron. Dev.* **37** 428

[9] Boyle D S, Govender K and O'Brien P 2002 *Chem. Commun.* **1** 80

[10] Zhong W Z and Hua S K 1999 *Morphology of Crystal Growth* (Beijng: Science Press) p336 (in Chinese)

[11] Li W J, Shi E W, Zhong W Z *et al* 1999 *J. Cryst. Growth* **203** 186

[12] Wang B G, Shi E V, Zhong W Z *et al* 1997 *J. Chin. Ceram. Soc.* **25** 223 (in Chinese)

[13] Wang B G, Shi E V, Zhong W Z *et al* 1997 *Chin. Sci. Bull.* **42** 1143 (in Chinese)

[14] Shi S C *et al* 2004 *Chin. J. Lumin.* **25** 272 (in Chinese)

[15] Chris G, Van de Walle 2001 *Physica* B **308–310** 899

[16] Xu P S, Sun Y M, Shi C S, Xu F Q and Pan H B 2003 *Nucl. Instrum. Methods Phys. Res.* B **199** 286

[17] Vanheusden K, Seager C H, Warren W L, Tallant D R and Voigt J A 1996 *Appl. Phys. Lett.* **68** 403

[18] Liu Y C, Zhang X T, Zhang J Y *et al* 2002 *J. Lumin.* **6** 563 (in Chinese)

[19] Zhang S B, Wei S H and Zunger A 2001 *Phys. Rev.* B **63** 075205

[20] Chen Y, Bagnall D M, Zhu Z *et al* 1997 *J. Cryst. Growth* **181** 165